INTEGRATED FIELD RESEARCH CHALLENGE SITE
Hanford 300 Area

U.S. Department of Energy Office of Science
Environmental Remediation Sciences Program

Integration of Core, Log, and Electrical Resistivity Tomography Data to Improve Hydrogeological Characterization of the Hanford 300 Area IFRC Site

Andy Ward[1], Roelof Versteeg[2], Tim Johnson[2], Jason Greenwood[1], and Kate Draper[1]

[1]Pacific Northwest National Laboratory, Richland, WA 99354; [2]Idaho National Laboratory, Idaho Falls, ID 83402

Background: Owing to the depositional environment, flow and transport properties at the 300 Area IFRC site show significant anisotropy and heterogeneity. Development of successful remediation strategies requires characterization of these properties, their spatial and directional dependence at relevant scales.

Objective: To develop lab-validated interpretation tools for mapping the 3-D distribution of transport properties.

Approach: Advanced geological analyses, reservoir-characterization tools, and workflows linked, with comprehensive data management protocols and inverse modeling, that have proven successful in oil field research, are being applied to the shallow unconsolidated formations typical of DOE waste sites (Fig.1).

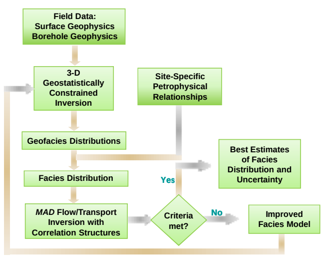

Fig. 1. Workflow for Integrated Site Characterization

Petrophysical Relationships

- ► Characterize particle size distributions (psd), shape indices (sphericity and angularity), and packing efficiencies of end- members and representative facies from the IFRC Site
- ► Establish relationships between psd moments, facies geometric, transport, and geophysical properties as the basis of 3-D model parameterization

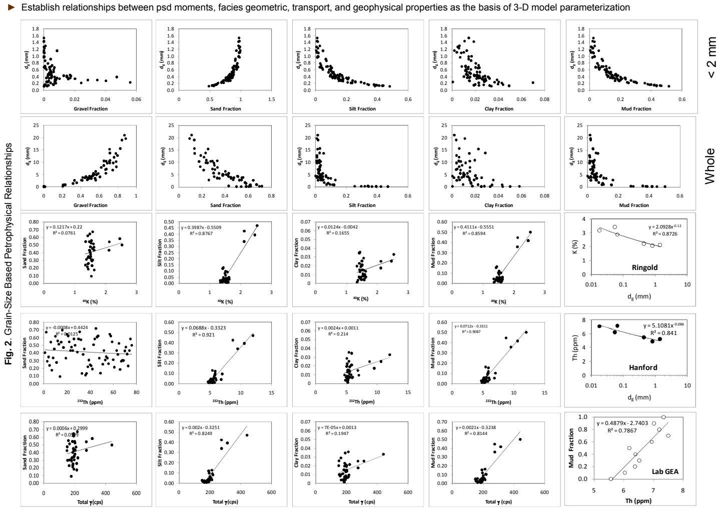

Fig. 2. Grain-Size Based Petrophysical Relationships

Characterizing Heterogeneity with Electrical Resistivity

Fig. 3. IFRC well field showing surface and subsurface electrode arrays

Resistivity Monitoring Array

The 28 instrumented IFRC wells are shown in Fig. 3. Each well is instrumented with 15 permanent electrodes in the vadose zone and 15 removable electrodes in the saturated zone, for a total of 840 electrodes. Electrodes are evenly spaced at 0.6-m intervals, to a depth of 18 m, the approximate depth of the Hanford/Ringold contact. There are 148 surface electrodes installed with telescoping radii from 5 to 40 m on 15° rotations about the center.

Data Acquisition

Resistivity data were collected using an 8-channel ERT system. Five 8-well 3D surveys were required to cover the site, with overlapping wells between adjacent surveys to provide data continuity. Full reciprocal measurements were collected for error analysis and data filtering. Accepted reciprocal measurements were averaged so that after filtering the data set comprised 50,295 measurements.

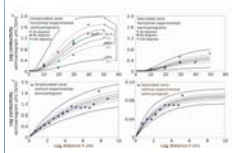

Fig. 5. Borehole EMI-based experimental semivariograms

Geostatistical Analysis

We used EM borehole induction logs to compute experimental semivariograms in each of the three horizontal directions corresponding to the triangular alignment of the well field, and also in the vertical direction (Fig. 5). The experimental values are modeled with Gaussian and spherical semivariograms. Confidence intervals are generated by selecting a mean and standard deviation of the sill and range such that the resulting distribution of semivariograms adequately bounds the experimental values. For each inverse realization, a set of semivariograms is randomly chosen from these distributions, and used to constrain the realization.

Example Realizations

INL's parallel inversion code (Johnson et al. 2010) was used to invert resistivity on an unstructured tetrahedral mesh consisting of 73,793 nodes and 460,926 elements. Fig. 6 shows three realizations from the geotatistically constrained inversion algorithm. The target horizontal and vertical semivariograms sampled from the semivariogram distributions, and the corresponding fit to those semivariograms are shown in the first two columns. The third column shows the resistivity fit in terms of residual error. The fourth column shows the boundaries of the bulk conductivity structure at the IFRC well-field.

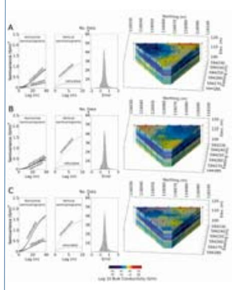

Fig. 6. Three of 100 realizations from the Geostatistically Constrained Inversion Algorithm

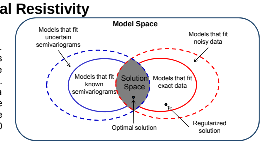

Fig. 4. Model space for Geostatistically Constrained Inversion

Geostatistically Constrained Inversion

Resistivity data are typically inverted using regularization (i.e. smoothness) constraints to remove the ill-posedness. The two main limitations of regularized inversion are 1) solutions are smoothed according to the data resolution, 2) uncertainty estimates are difficult to produce. These limitations are addressed through geostatistically constrained inversion. Inverse solutions are sampled from the space of solutions honoring the resistivity measurements (with noise) and the estimated (and uncertain) spatial covariance structure. If the data noise and uncertainty in the spatial covariance structure are not under-estimated, then the "true" solution belongs to this space. By repeatedly sampling models from this space, we generate a suite of maximum likelihood models which can be used estimate solution uncertainty through ensemble statistical analysis (Fig. 4).

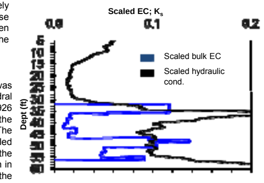

Fig. 8. Relationship between Scaled EC_b and Scaled EBF K_s

Uncertainty Estimation

The regularized solution and the mean show similar structural characteristics, but the mean displays greater laterally continuity and resolution (e.g. the water table at ~ 105 m) elevation (Fig. 7). The standard deviation summarizes the uncertainty about the mean. As expected, the deviation is greater in regions with low data sensitivity (e.g. the surface) and regions with larger sill values and high spatial covariance uncertainty (e.g. the vadose zone).

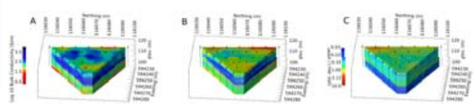

Fig. 7. (A) regularized solution, (B) ensemble mean, and (C) ensemble deviation of 100 geostatistically constrained inversions.

Characterizing Anisotropy with Electrical Resistivity

Azimuthal Resistivity Monitoring Array

A generalized array of azimuthal electrodes was constructed with seven telescoping radii of 5 to 40 m with 15° rotations between each of the 169 electrodes (Figure 10). Each electrode was connected to the MPT-DAS1 8-channel system (Multiphase Technologies, Sparks, NV) with a capacity for multiplexing 256 electrodes. Arrow, Square and 3D tomography type arrays with exploration depths of up to 36 m were acquired.
ARS data were processed with spectral, elliptical fitting, and directional statistical methods to quantify horizontal anisotropy and heterogeneity at each exploration depth (Fig. 11)..

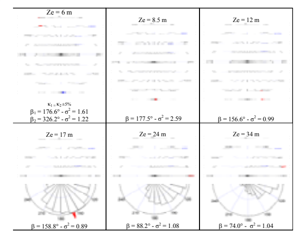

Fig. 9. Rose diagrams showing azimuths for the arrow array.

Results

The primary findings are that:

1) the arrow array is more sensitive than the square array to known formation boundaries;
2) ARS response within the braided fluvial deposits of the Hanford Formation are controlled by anisotropy with a minimal influence of heterogeneity at the IFRC site ($\psi < 1$);
3) the Hanford Formation I_a ranges between 1.03 and 1.53 with a preferred orientation β between 146.2° -178° with σ_{max}=1.61°;
4) the electrical anisotropy strike direction in the Hanford Formation is consistent with the orientation of a preferred path inferred from tracer experiments;
5) ARS is sensitive to the location of the vertical contact between the Hanford and Ringold Formations (17-m) as well as the strike (159°) of an incision feature at this boundary which influences flow.

These results indicate that ARS with the arrow array and associated processing methods can be used to rapidly and noninvasively delineate preferential flow directions of groundwater within the shallow aquifer at the IFRC site.

Conclusions

- ► Grain size moments provide a good basis for relating properties across well field
- ► Clay, silt, and sand mass vary with dg and So; clay is least sensitive due to low %
- ► Spectral gamma response is controlled by fine-fraction and can be used to propagate grain size moments across well field
- ► The capability to model and invert electrical geophysical data in a parallel computing environment allows full utilization of current resistivity/IP data collection capabilities, and significantly improves the capability to characterize the electrical geophysical properties of the subsurface, and to monitor spatiotemporal variations in electrical geophysical properties caused by evolving subsurface processes.
- ► The limitations of current resistivity inversion methods are overcome by geostatistically constrained inversion whose solutions are sampled from the space of solutions honoring the resistivity measurements (with noise) and the estimated (and uncertain) spatial covariance structure
- ► Surface surveys like ARS can compliment ERT surveys to provide information on effective properties.

Scientific Opportunities For Research

- ► Improved understanding of KUT response and develop generalized model for other sites
- ► Quantify temporal changes in the flow field and transport properties resulting from river stage fluctuations
- ► Geophysics based estimation of hydrological properties through the use of electrical geophysical and hydrological time-lapse data
- ► Development, validation and application of coupling between a Spectral IP geophysical forward and inverse code and a reactive transport model to enhance both characterization results as well as the spatiotemporal monitoring of precipitation/dissolution
- ► Development of an integrated, consistent core to field scale description and understanding of the distribution and interrelation between hydrological, geochemical and geophysical properties

PNNL-SA-70923